論文 / 著書情報
Article / Book Information

論題(和文)	アンボンドPCaPC造壁の構造性能評価(その 1 実験概要及び実験結果)
Title(English)	Evaluation of Structural Performance of Unbonded Post-tensioned Precast Concrete Walls (Part I: Experimental Program and Results)
著者(和文)	Rajbhandari Priyana, 張 明嘉, 植村 一貴, 小原 拓, 河野 進, MUKAI David Jiro, 谷 昌典
Authors(English)	Priyana Rajbhandari, Meika Cho, Kazuki Uemura, Taku Obara, Susumu Kono, David Mukai, Masanori Tani
出典(和文)	日本建築学会大会学術講演梗概集, , , pp. 717-718
Citation(English)	Summaries of technical papers of annual meeting, AIJ, , , pp. 717-718
発行日 / Pub. date	2021, 9
権利情報	一般社団法人 日本建築学会

Evaluation of Structural Performance of Unbonded Post-tensioned Precast Concrete Walls (Part I: Experimental Program and Results)

Rocking wall
Unbonded post-tensioning
Self-centering

○Priyana RAJBHANDARI[1] Meika CHO[1] Kazuki UEMURA[1]
Taku OBARA[1] Susumu KONO[1] David MUKAI[2]
Masanori TANI[3]

1 Introduction

Present society requires buildings to maintain their functionality in addition to securing human lives after seismic events. Details from past earthquakes have shown that the functionality of buildings can be disturbed even if the structural elements are not damaged[1)]. In order to address this issue, unbonded post-tensioned precast concrete walls (hereafter, rocking walls) have been proposed as a solution. After Priestley and Tao[2)] studied the use of rocking system in a precast frame building, qualitative researches have been carried out on this topic and the first technical guideline for seismic design of ductile jointed precast concrete structures was published in 2006[3)]. Despite the advances, relatively a small number of new buildings incorporate rocking walls and further research is needed to accelerate the implementation of these walls into practice[4)]. In this study, experiments on four rocking walls have been conducted to clarify the behavior under lateral load. Part I presents outline of the experiment and obtained results such as load-drift relationship and strain distribution in PT rod.

2 Experimental Program

2.1 Specimen details

Specimens consisted of four rectangular cross-section rocking walls subjected to quasi-static cyclic loading. Two specimens represented non-structural walls with axial force ratio as a variable (PCNW1, PCNW2) and the other two represented structural walls with wall thickness as a variable (PCW1, PCW3). Geometry and reinforcement details are shown in Figure 1.

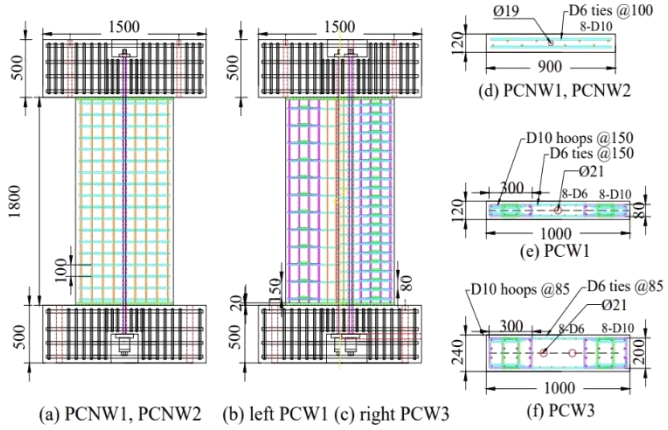

Fig.1: Geometry and reinforcement detail (unit: mm)

A 20mm thick mortar bedding was placed between wall panel and the stubs. Specimen properties and detailed bar arrangement are described in Table 1. Table 2 and Table 3 show the mechanical properties of concrete and steel reinforcement, respectively.

Table 1: Specimen details

Specimen name	PCNW1	PCNW2	PCW1	PCW3
Concrete design strength	35MPa			
Wall height*length	1800mm*900mm		1800mm*1000mm	
Wall thickness	120mm		120mm	240mm
Longitudinal reinforcement in confinement			8-D10	16-D10
Longitudinal reinforcement	8-D10		8-D6	
Lateral reinforcement in confinement			4-D10	
Lateral reinforcement	2-D6		2-D6	
PT rod	1- Ø19		1- Ø21	2- Ø21
External axial force ratio	0.050	0.300	0.100	0.100
Prestressing ratio	0.055	0.055	0.060	0.060
Total axial force ratio	0.105	0.355	0.160	0.160

Table 2: Mechanical properties of concrete

Specimen	Compressive strength (MPa)	Compressive peak strain (%)	Tensile strength (MPa)	Young's modulus (GPa)
PCNW1	37.1	0.310	2.88	22.7
PCNW2	40.9	0.257	3.00	26.7
PCW1	38.5	0.256	2.76	24.8
PCW3	39.4	0.254	2.68	26.6

Mortar compressive strength: 90 MPa

2.2 Loading setup

A schematic of test setup is shown in Figure 2. A steel frame, not shown, was placed adjacent to the wall to prevent out of plane deformation. Axial load and lateral load was applied with two vertical hydraulic jacks and one horizontal jack respectively via a loading beam. Since non-structural walls usually interact with frame resulting in certain degree of anti-symmetric bending when

loaded laterally, PCNW1 and PCNW2 were loaded in double curvature whereas PCW1 and PCW3 were loaded as cantilever walls. Northward drift is considered positive. Horizontal cyclic displacement with constant axial load was applied two cycles at each limit drift of ±0.125%, ±0.25%, ±0.5%, ±0.75%, ±1%, ±1.5%, ±2%, ±3%, ±4%. After that, monotonic loading was applied on positive direction till failure.

Table 3: Mechanical properties of steel

Tag	Yield strength (MPa)	Tensile strength (MPa)	Young's modulus (GPa)	Yield strain (%)
D6	369※1	544	194	0.398※1
D6 spiral	489	576	199	0.246
D10	357	501	187	0.192
Ø19	1192※1	1295	209	0.770※1
Ø21	1207※1	1290	197	0.812※1

※1: 0.2% offset proof stress and strain
At 0.02% offset strain, strain of Ø19 and Ø21: 0.572%,0.563%
strength of Ø19 and Ø21: 1143 MPa, 1063MPa

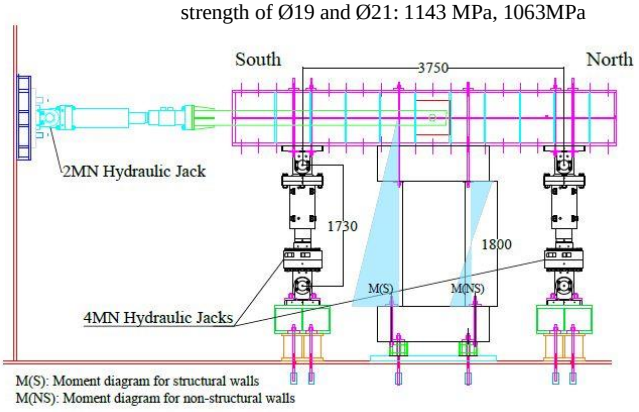

Fig. 2. Loading system (unit: mm)

3 Experimental results

3.1 Shear force-drift relationship

The lateral load-drift responses are shown in Figure 3. For PCNW1, the maximum capacity was reached at R=1.5% in both positive and negative drift. PT rod yielded after that at R=+2.6/-2%. PCNW2 was loaded under high axial force ratio. Its maximum load capacity, observed at R=0.25%, was increased by a factor of 1.6-1.7 as compared to PCNW1 and the post peak backbone curve degraded quickly due to vertical splitting cracks. In both non-structural walls, loading was terminated because axial load couldn't be maintained.

The response for structural walls was nearly non-linear elastic with good self-centering capability. PCW1 reached its maximum capacity at R=+1.45/ -0.96% and PT rod didn't yield. PCW3, which had thicker section than PCW1, achieved about two times larger maximum capacity at R=+2.88/-1.44%.

After the PT rods reached their elastic limit, stiffness degradation became more apparent and energy dissipation was observed with increase in drift. High deterioration of load carrying capacity was observed in non-structural walls as compared to structural walls. This is due to the excessive concrete crushing in non-structural walls.

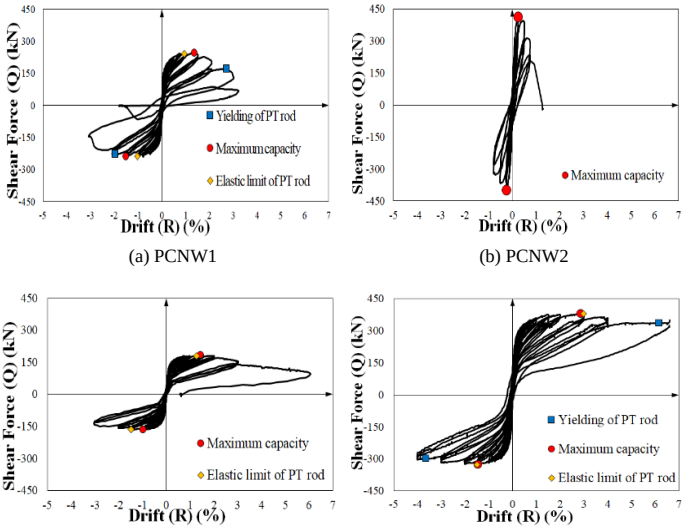

(a) PCNW1 (b) PCNW2

(c) PCW1 (d) PCW3

Fig. 3. Shear force, Q – drift, R relationship

3.2 PT rod strain-drift relationship

Strain on PT rods at each drift is shown in Figure 4. Of all the specimens, one PT rod of PCW3 reached the highest strain of 0.99% at R=6.60% whereas PT rod of PCNW1 reached the elastic strain limit corresponding to 0.02% offset strain[1)] earliest at R=+1.52/-1.40%.

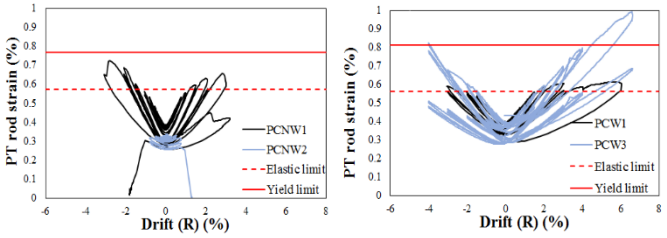

(a) Non-structural walls (b) Structural walls

Fig. 4. PT rod strain – drift relationships

4 Conclusion

Four specimens representing non-structural and structural rocking walls built with no energy dissipating system were tested under axial and cyclic lateral loading. The overall behavior of structural walls was good with no significant strength degradation in lower drifts and they exhibited good self-centering capability. However the load carrying capacity of non-structural walls degraded swiftly after they reached their maximum capacity.

References and acknowledgement are in part III of this paper.

[1] 東京工業大学
[2] ワイオミング大学
[3] 京都大学

[1] Tokyo Institute of Technology
[2] University of Wyoming
[3] Kyoto University